Arch Toxicol
DOI 10.1007/s00204-016-1835-3

ORGAN TOXICITY AND MECHANISMS

# Bilirubin-induced ER stress contributes to the inflammatory response and apoptosis in neuronal cells

**Mohammed Qaisiya[1] · Cristina Brischetto[1] · Jana Jašprová[2] · Libor Vitek[2,3] · Claudio Tiribelli[1,4] · Cristina Bellarosa[1]**

Received: 25 February 2016 / Accepted: 24 August 2016


**Abstract** Unconjugated bilirubin (UCB) in newborns may lead to bilirubin neurotoxicity. Few studies investigated the activation of endoplasmic reticulum stress (ER stress) by UCB. We performed an in vitro comparative study using undifferentiated SH-SY5Y, differentiated GI-ME-N neuronal cells and human U87 astrocytoma cells. ER stress and its contribution to inflammation and apoptosis induced by UCB were analyzed. Cytotoxicity, ER stress and inflammation were observed only in neuronal cells, despite intracellular UCB accumulation in all three cell types. UCB toxicity was enhanced in undifferentiated SH-SY5Y cells and correlated with a higher mRNA expression of pro-apoptotic CHOP. Mouse embryonic fibroblast knockout for CHOP and CHOP siRNA-silenced SH-SY5Y increased cells viability upon UCB exposure. In SH-SY5Y, ER stress inhibition by 4-phenylbutyric acid reduced UCB-induced apoptosis and decreased the cleaved forms of caspase-3 and PARP proteins. Reporter gene assay and PERK siRNA showed that IL-8 induction by UCB is transcriptionally regulated by NFκB and PERK signaling. These data suggest that ER stress has an important role in the UCB-induced inflammation and apoptosis, and that targeting ER stress may represent a potential therapeutic approach to decrease UCB-induced neurotoxicity.

**Keywords** Bilirubin neurotoxicity · ER stress · 4-PBA · CHOP · NFκB

✉ Mohammed Qaisiya
m.qaisiya@csf.units.it

[1] Fondazione Italiana Fegato ONLUS, Italian Liver Foundation ONLUS, AREA Science Park Basovizza Bldg Q, 34149 Trieste, Italy

[2] Institute of Medical Biochemistry and Laboratory Medicine, 1st Faculty of Medicine, Charles University in Prague, 12000 Prague, Czech Republic

[3] 4th Department of Internal Medicine, 1st Faculty of Medicine, Charles University in Prague, 12000 Prague, Czech Republic

[4] Department of Medical Sciences, University of Trieste, 34149 Trieste, Italy

## Introduction

Elevated level of unconjugated bilirubin (UCB) is responsible for the clinical manifestation of neonatal jaundice. In most cases, this is a transient phenomenon without any clinical consequences. When hyperbilirubinemia is prolonged and severe, abnormal accumulation of bilirubin may lead to bilirubin encephalopathy or to a more severe condition (kernicterus) characterized by irreversible neurological sequelae (Shapiro 2004; Watchko and Tiribelli 2013). At the molecular level, several studies showed the effects of UCB toward plasma membrane, mitochondria, endoplasmic reticulum (ER), calcium homeostasis and redox state (Watchko 2006). Among the different cellular compartments, ER has an important role in UCB metabolism. Once entered the cell, UCB is bound to ligandins and shuttled directly to the ER. In the hepatocyte, ER is the site of bilirubin conjugation by UGT1A1 (Kamisako et al. 2000). When bilirubin glucuronidation capacity is reduced or absent, bilirubin oxidation by cytochrome P450 enzymes, that are localized primarily in the membrane of ER (Neve and Ingelman-Sundberg 2010), has been suggested to significantly contribute in the elimination of the pigment (Abu-Bakar 2005; Gambaro et al. 2016).

The ER is a highly dynamic organelle, and its complex functions can be significantly influenced by a multitude of parameters both inside the cell and in its

Published online: 30 August 2016

microenvironment (Schönthal 2012). When cells are exposed to stimuli that rupture the protein folding mechanism, ER stress occurs and cells activate a signaling pathway defined as unfolded protein response (UPR) that determine cell fate (Malhotra and Kaufman 2007; Tsang et al. 2010; Walter and Ron 2011). The UPR consists of three main membrane-associated proteins as PKR-like ER Kinase (PERK), inositol requiring enzyme 1 (IRE-1) and activating transcription factor 6 (ATF6). Stress conditions result in the recruitment of a chaperon called glucose-related protein 78 (GRP78) away from UPR sensors and their activation. Activated PERK leads to a general inhibition of translation (through eIF2α phosphorylation) with specific induction of the transcription factors ATF3, ATF4 and CHOP, while IRE-1 and ATF6 generate an active transcription factors XBP1-spliced and ATF6 (after its cleavage in Golgi), respectively (Lai et al. 2007; Schröder and Kaufman 2005). The primary role of UPR is to restore ER homeostasis and provide cell survival. However, under sustained and irreversible ER stress, a switch to pro-apoptotic signaling occurs (Urra et al. 2013), where caspases-3 activation and CHOP induction play a critical role in ER stress-mediated apoptosis (Hitomi et al. 2004; Zinszner et al. 1998; Oyadomari and Mori 2004). Furthermore, ER stress is associated with several events that contribute to cell injury such as oxidative stress and inflammation (Chaudhari et al. 2014). Chronic ER stress elicits inflammatory response through complex mechanisms (Hasnain et al. 2012) that include the induction of several cytokines and NFκB activation as one of the key player (Hotamisligil 2010; Garg et al. 2012).

We have previously described the induction of ER stress genes in SH-SY5Y neuronal cells treated with a toxic dose of bilirubin (Calligaris et al. 2009). We subsequently observed the induction of ATF3 mRNA after 4 h of UCB exposure, representing the earliest response to UCB insult (Qaisiya 2014). Elevated concentration of UCB causes the induction of ER stress markers in hepatic-derived cells (Oakes and Bend 2010; Müllebner et al. 2015) and oligodendrocyte precursor cells (Barateiro et al. 2012). Other in vitro studies demonstrated the induction of inflammatory response genes by UCB through the cytokine receptors and NFκB activation in primary culture of neurons (Falcão et al. 2006) and microglia (Brites 2012), while in astrocytes the results are still controversial (Brites 2012; Yueh et al. 2014). The involvement of cytokine receptor activation by UCB is confirmed in an in vivo study where the absence of Toll-like receptor 2 blocked the induction of TNFα and IL-6 (Yueh et al. 2014).

Until now, no evidence is available regarding the contribution of ER stress in mediating inflammatory response or cell death induced by UCB. In the present work, we performed an in vitro comparative study using two human neuronal cell lines (undifferentiated SH-SY5Y cells and differentiated GI-ME-N cells) and one human astrocytoma cell line (U87 cells) to study the effects of UCB toward cell toxicity, ER stress and inflammation. We also analyzed the signaling pathways that linked ER stress to inflammation and the contribution of ER stress to apoptosis.

## Materials and methods

### Cell cultures

SH-SY5Y neuroblastoma cells were maintained in EMEM/F12 1:1 medium supplemented with 15 % fetal bovine serum (FBS). Human NB cell line (defined as GI-ME-N) comes from the Bank of Biological Material Interlab Cell Line Collection, Advanced Biotechnology Center, Genoa, Italy, and were kindly provided by Dr. Mariapaola Nitti. They were maintained in RPMI 1640 medium, supplemented with 10 % FBS. U87 astrocytoma cells were maintained in DMEM medium supplemented with 10 % FBS. Mouse embryonic fibroblasts (MEF) knockout for CHOP (CHOP KO) (Zinszner et al. 1998) were kindly provided by Prof. Patrizia Agostinis Laboratory of Cell Death Research and Therapy, Belgium. MEF cells were maintained in DMEM high-glucose medium supplemented with 10 % FBS. All media were supplemented with 1 % penicillin/streptomycin solution (100 U/mL penicillin, 100 mg/mL streptomycin), 2 mM L-glutamine and 1 % nonessential amino acids (Sigma–Aldrich, USA).

### Treatments

Because UCB toxicity is related to the amount of the free bilirubin (Bf) (Ahlfors et al. 2009) and considering that the threshold value of bilirubin toxicity in vitro occurs at Bf of 70 nM (Ostrow et al. 2003), cells at 80 % of confluence were treated with toxic Bf concentration (140 or 300 nM) for the indicated time. UCB dissolved in DMSO (3 μg/μL) was added to complete cell medium, and its concentration was verified spectrophotometrically at 468 nm. The Bf concentration was calculated according to protocol described by Roca et al. (Roca et al. 2006). Control experiments were performed by exposing the cells to the same final concentration of DMSO. Phenylbutyric acid (4-PBA, Sigma Aldrich) was prepared by titrating equimolecular amount of 4-PBA with sodium hydroxide to pH 7.4. SH-SY5Y cells were pretreated with 2 mM of 4-PBA for 2 h and then treated with 0.6 % DMSO or 140 nM Bf for additional 8 or 24 h in the presence of 4-PBA. Thapsigargin (Sigma Aldrich) was used at 2 μM final concentration as a positive control to induce ER stress. Pyrrolidinedithio carbamate ammonium (PDTC,

**Table 1** List of human primer sequences used for qRT-PCR analysis

| Gene | Accession number | Forward primers 5′–3′ | Reverse primers 5′–3′ |
|---|---|---|---|
| CHOP | NM_001195056 | CACTCTCCAGATTCCAGTCAG | AGCCGTTCATTCTCTTCAGC |
| XBP1 | NM_005080 | ATGGATTCTGGCGGTATTG | CTGGGTCCTTCTGGGTAG |
| ATF6 | NM_007348 | CAGAGAACCAGAGGCTTA | TGCTCATAGGTCCATAGTT |
| GRP78 | NM_005347 | GCACAGACAGATTGACCTATTG | GTAGCACAGGAGCAC |
| NFκB (p65) | L19069 | GAATGCTGTGCGGCTCTG | CACGATTGTCAAAGATGGGATG |
| TNFα | NM_000594 | CCTGACATCTGGAATCTGGAG | AGGAAGTCTGGAAACATCTGG |
| IL-8 | NM_000584 | GACATACTCCAAACCTTTCCAC | CTTCTCCACAACCCTCTGC |
| GAPDH[a] | NM_002046.4 | TCAGCCGCATCTTCTTTTG | GCAACAATATCCACTTTACCAG |
| HPRT[a] | NM_000194 | ACATCTGGAGTCCTATTGACATC | CCGCCCAAAGGGAACTGATAG |

[a] Housekeeping genes used to normalize the expression of target genes

Sigma–Aldrich) was used as a selective NFκB inhibitor. SH-SY5Y cells were pre-treated with 100 µM of PDTC for 2 h to and then treated with 0.6 % DMSO, 140 nM Bf and 100 ng/mL lipopolysaccharide (LPS, Sigma–Aldrich) for additional 8 h in the presence of the inhibitor.

### Quantification of intracellular UCB level

SH-SY5Y, GI-ME-N and U87 cells at 80 % confluence were incubated with 140 nM Bf for 4, 8, and 24 h, or 0.6 % DMSO. After treatment time, cells were collected by centrifugation and washed three times in PBS. Intracellular UCB level was quantified using method of high-performance liquid chromatography with diode array detector (Agilent, Santa Clara, USA) according to Zelenka (Zelenka 2008). Briefly, cells were suspended with physiological solution, sonicated and mixed with internal standard (mesobilirubin). This solution was extracted with methanol/chloroform/hexan (10/5/1, v/v/v) at pH 6.2. The lower phase was transferred into new vial that contained hexane and carbonate buffer (pH 10). The resulting polar droplet was loaded onto Luna C-8 reverse phase column (Phenomenex, Torrance, USA), and separated pigments were detected at 440 nm. Protein concentration in the cell suspension was determined by DC protein assay (Bio-Rad, USA), and results were expressed as nmol/mg of protein. All steps were performed at dim light.

### Analysis of cell viability and toxicity

Cells toxicity was determined by the mean of LDH release using CytoTox-oneTM homogenous membrane integrity assay (Promega, USA) following the manufacturer's instructions. Percent of dead cells were calculated relative to cells treated with lysis buffer to obtain 100 % of LDH release. Cells viability were determined by 3(4,5-dimethylthiazolyl-2)-2,5 diphenyl tetrazolium (MTT) assay according to manufacturer's instructions.

### Western blot

Total proteins were extracted by lysing the cells in ice-cold cell lysis buffer (Cell Signaling Technology, USA). Protein concentration was determined by the bicinchoninic acid protein assay (BCA) according to manufacturer's instructions. Equal amounts of protein were separated by 12 % SDS–polyacrylamide gel electrophoresis (SDS-PAGE) and transferred to PVDF membranes (Bio-Rad Laboratories). Membranes were blocked in 5 % milk or 4 % BSA in T-TBS (0.2 % Tween 20, 20 mM Tris–HCl (pH 7.5) and 500 mM NaCl) and incubated overnight at 4 °C with primary antibodies: anti GRP78 (Santa Cruz Biotechnology, Inc sc-13968), anti ATF-6α (Santa Cruz Biotechnology, Inc sc-166659), anti-caspase-3 (Cell Signaling Technology, #9662), anti-PARP p85 fragment (Promega, Italy G7341) and anti-actin (Sigma–Aldrich, A2066). Membranes were then incubated with anti-rabbit or anti-mouse HRP-conjugated secondary antibody (Dacko Laboratories, Denmark). Protein bands were detected by peroxide reaction using ECL Plus Western Blot detection system solutions (ECL Plus Western Blot detection reagents, GE-Healthcare Bio-Sciences, Italy). The relative intensities of protein bands were analyzed using the NIH Image software (Scion Corporation Frederick, MD, USA), normalized to α-actin and represented as relative to controls.

### Quantitative real-time PCR and ELISA

RNA extraction, cDNA synthesis and real-time PCR (qRT-PCR) were performed as previously described (Qaisiya 2014). Primers used were listed in Table 1. Expression was normalized to housekeeping genes and expressed as relative to cells treated with DMSO in the absence or presence or inhibitors when applied. After UCB incubation, SH-SY5Y supernatants were used to quantify IL-8 and TNFα protein using Instant ELISA Kit (eBioscience) according to the manufacturer's protocol.

### PERK and CHOP small interference RNA

The experimentally validated PERK siRNA (SI02223718, Qiagen, USA) and CHOP siRNA (SI00059528, Qiagen) were used to knockdown PERK and CHOP expression. siRNA against nontarget mRNA (1027310, Qiagen) was used as negative control. siRNA was transfected using siLentFect™ Lipid reagent (Bio-Rad laboratories, Italy) according to the manufacturer's recommendation. SH-SY5Y cells at 60 % confluence were transfected with 3 µL siLentFect reagent (mock) or 50 nM of siRNAs in the presence of 3 µL siLentFect reagent for 48 h, and siRNA efficiency was analyzed by qRT-PCR. For UCB treatment, after 48 h siRNA transfection cells were treated with 0.6 % DMSO or 140 nM Bf for additional 8 or 24 h. Results were expressed as relative to Ct siRNA transfected cells treated with UCB.

### NFκB luciferase reporter gene assay

The constructs of human IL-8 promoter, 1498/+ 44 hIL-8/Luc and 162/+ 44 hIL-8 ΔNFκB/Luc were kindly received by Prof. Gianluca Tell (University of Udine, Italy) (Cesaratto 2013). One day before transfection, SH-SY5Y cells were seeded in triplicate in 96-well plates at 80 % confluence, then cells were transiently transfected with 400 ng of total DNA/well of (hIL-8/Luc promoter constructs and pRL-CMV Renilla luciferase constructs in a ratio of 49:1), using Lipofectamine™2000 reagent (0.8 µL) (Invitrogen, Carlsbad, CA) according to the manufacturer's instructions. The transfection reagent was removed 8 h post-transfection, and cells were incubated with complete medium for 24 h. The following day, cells were washed with PBS and then treated with 0.6 % DMSO, 140 nM Bf or 100 ng/mL lipopolysaccharide (LPS, Sigma–Aldrich) as positive control. Finally, cells were lysed and analyzed by Dual Luciferase Reporter Gene Assay Kit (KA3784, Abnova, Taiwan) according to the manufacturer's instructions. The luminescence signals were quantified using a Perkin Elemer EnSpire multiplate reader (PerkinElmer, USA). Firefly luciferase activity was normalized to the Renilla luciferase activity.

### Statistical analysis

GraphPad Prism software was used to perform statistical analysis. Data were obtained from at least three independent experiments and are expressed as mean ± SD. Analysis was performed using student's *t* test. $P < 0.05$ was considered as significant.

## Results

### UCB induces differential cellular toxicity despite comparable intracellular accumulation

In the present study, we used undifferentiated SH-SY5Y neuronal cells, differentiated GI-ME-N neuronal cells and astrocytoma U87 cells. The cytotoxic effects of UCB was assessed by LDH assay after exposing the three cell lines to increasing concentrations of free bilirubin: 40 nM Bf (non-toxic), 140 nM Bf or 300 nM Bf (toxic). SH-SY5Y cells showed 25 and 70 % of LDH-based cytotoxicity when treated with 140 nM Bf or 300 nM Bf, respectively, while GI-ME-N cells showed about 30 % of cytotoxicity at both concentrations. U87 cells did not exhibit any significant change of LDH release at any toxic concentration (Fig. 1a). To measure UCB intracellular accumulation, SH-SY5Y, GI-ME-N and U87 cells were exposed to 140 nM Bf for 4, 8 and 24 h, and the intracellular UCB content was quantified by HPLC. Compared to 4 h, SH-SY5Y, GI-ME-N and U87 cells showed 1.8-folds, 3.0-folds and 1.9-folds increase at 8 h, respectively, and 3.8-folds, 4.8-folds and 2.4-folds at 24 h, respectively (Fig. 1b).

### UCB induces ER stress only in neuronal cells

We analyzed the mRNA expression of ER stress-related genes in the three cell lines exposed to 140 nM Bf for 4, 8 and 24 h. Compared to DMSO-treated cells, SH-SY5Y cells treated with UCB showed an induction of CHOP (sixfolds) at 4 h, followed by the induction of ATF6 (twofolds) and GRP78 (fourfolds) at 8 h. The up-regulation of all genes was maintained until 24 h. GI-ME-N cells showed an up-regulation of CHOP (19-folds), ATF6 (sixfolds) and GRP78 (fivefolds) after 4 h of UCB exposure which was maintained till 24 h. No changes were detected in U87 cells exposed to 140 nM Bf at either 8 or 24 h (Table 2). GRP78 protein expression and ATF6 proteolytic cleavage were evaluated in the three different cell lines. If compared to SH-SY5Y cells (onefold), the basal expression of GRP78 protein is higher in U87 cells (12-folds) and in GI-ME-N (sevenfolds). UCB treatment induced GRP78 protein expression in SH-SY5Y cells (eightfold) and GI-ME-N cells (twofolds), while no induction was observed in U87 cells. Thapsigargin caused a 32.5-fold induction of GRP78 protein in SH-SY5Y cells (Fig. 2a, b). Cleaved ATF6 p50 protein was not induced by UCB treatment in the three cell types, while ATF6 p50 protein basal expression was threefold higher in U87 and GI-ME-N cells compared to SH-SY5Y cells (Fig. 2c, d). To confirm the induction of ER stress genes by UCB, we tested the effects of the ER

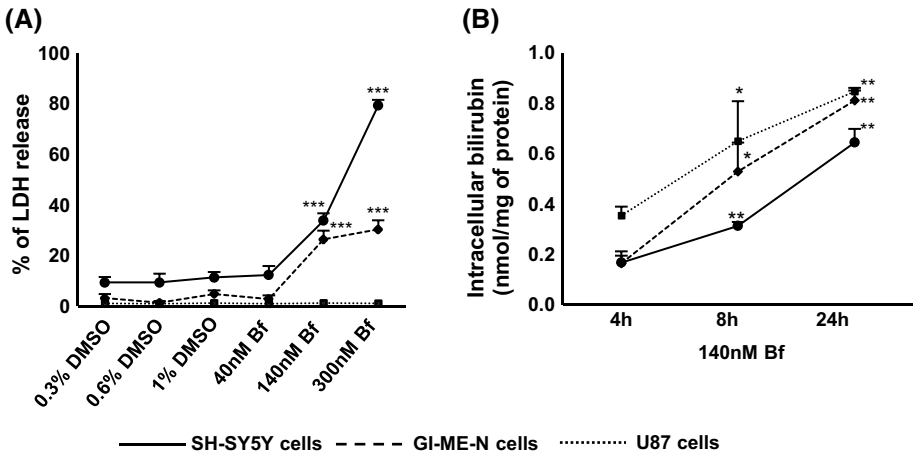


**Fig. 1** Effects of UCB exposure on LDH release and UCB accumulation in three different cell lines. **a** LDH release in SH-SY5Y, GI-ME-N and U87 cells treated with 40 nM Bf, 140 nM Bf or 300 nM Bf and the relative controls 0.3 % DMSO, 0.6 % DMSO or 1 % DMSO, respectively, for 24 h. Percent of dead cells was normalized to cells treated with lysis buffer (100 % of LDH release) and expressed as relative to controls. **b** Amount of intracellular UCB content in SH-SY5Y, GI-ME-N and U87 cells treated with 140 nM Bf for 4, 8 and 24 h. Cells treated with 0.6 % DMSO for 24 h were used as negative control (intracellular bilirubin content = 0). Significance relates to cells treated with UCB for 4 h. Data are the mean ± SD of four independent experiments (*$P < 0.05$, **$P < 0.01$, ***$P < 0.001$)

**Table 2** mRNA relative expression of ER stress-related genes

| Cell lines | Genes | 140 nM Bf (4 h) | 140 nM Bf (8 h) | 140 nM Bf (24 h) |
|---|---|---|---|---|
| SH-SY5Y cells | CHOP | 6 ± 0.8** | 46 ± 6** | 93 ± 9** |
| | ATF6 | 1.1 ± 0.1 | 2 ± 0.2* | 6 ± 0.2** |
| | GRP78 | 0.9 ± 0.2 | 4 ± 0.2** | 11 ± 1.3** |
| GI-ME-N cells | CHOP | 19 ± 5** | 22 ± 0.6*** | 6 ± 1.5** |
| | ATF6 | 6 ± 2** | 5.4 ± 0.9** | 8 ± 0.3** |
| | GRP78 | 5 ± 1.8* | 12 ± 3** | 5.5 ± 2* |
| U87 cells | CHOP | | 1 ± 0.2 | 0.7 ± 0.3 |
| | ATF6 | | 1 ± 0.2 | 0.9 ± 0.2 |
| | GRP78 | | 1 ± 0.1 | 1.1 ± 0.4 |

mRNA expression of CHOP, ATF6 and GRP78 in SH-SY5Y, GI-ME-N and U87 cell lines exposed to 140 nM Bf or 0.6 % DMSO for the indicated time. Expression is relative to cells treated with 0.6 % DMSO considered as 1. DMSO treatment has no effects on the expression of indicated genes at 8 and 24 h. Data are representative of the mean ± SD of four independent experiments (* $P < 0.05$, ** $P < 0.01$, *** $P < 0.001$)

stress inhibitor 4-PBA in SH-SY5Y cells. 4-PBA reduced the induction of GRP78, ATF6, XBP1 and CHOP by 55, 45, 65 and 67 %, respectively. 4-PBA reduced by 75 % the thapsigargin induction of GRP78 (Fig. 3).

## ER stress inhibition and CHOP knockout reduce cell susceptibility to UCB

Chronic ER stress is usually associated with cell injury and apoptosis. To assess if ER stress is involved in UCB cell toxicity, we treated SH-SY5Y cells with 140 nM Bf for 24 h in the presence of the ER stress inhibitor 4-PBA. LDH release was reduced from 31 to 10 % in the presence of 4-PBA (Fig. 4a). We then analyzed the levels of caspase-3, one of the key executioners caspases involved in apoptosis induced by ER stress (Hitomi et al. 2004) and cleaved poly (ADP-ribose) polymerase (PARP, p85 fragment), a well-known substrate for caspase-3 during apoptosis (O'Brien et al. 2001). Cleaved caspase-3 and cleaved PARP were undetectable in the DMSO-treated cells, while in the UCB treated cells, 4-PBA reduced their expression by 80 and 50 %, respectively (Fig. 4b, c). Several studies highlighted the role of CHOP in ER stress mediating cell toxicity. To assess its role in UCB toxicity, mouse embryonic fibroblasts (MEF) knockout for CHOP (CHOP KO) were exposed to 140 nM Bf or 2 µM thapsigargin for 24 h and cell viability analyzed by MTT test. Compared to DMSO-treated cells, UCB and thapsigargin reduced cells viability in CHOP WT cells to 72 and 50 %, respectively, while this was 91 and 70 % in CHOP KO cells (Fig. 4d). CHOP WT MEF exposed to 140 nM Bf for 24 h showed an up-regulation of CHOP mRNA, which was completely lost in the CHOP KO MEF cells (data not shown). To assess the role of CHOP in UCB-induced neurotoxicity, we transfected SH-SY5Y cells with CHOP siRNA and analyzed LDH release upon UCB exposure. CHOP siRNA (50 nM) down-regulated CHOP mRNA to about 55 % as compared to control siRNA (50 nM) (Fig. 4e). Upon UCB treatment, the percentage of LDH release was significantly reduced from 37 % in control siRNA-transfected cells to 22 % in CHOP siRNA-transfected cells (Fig. 4f).

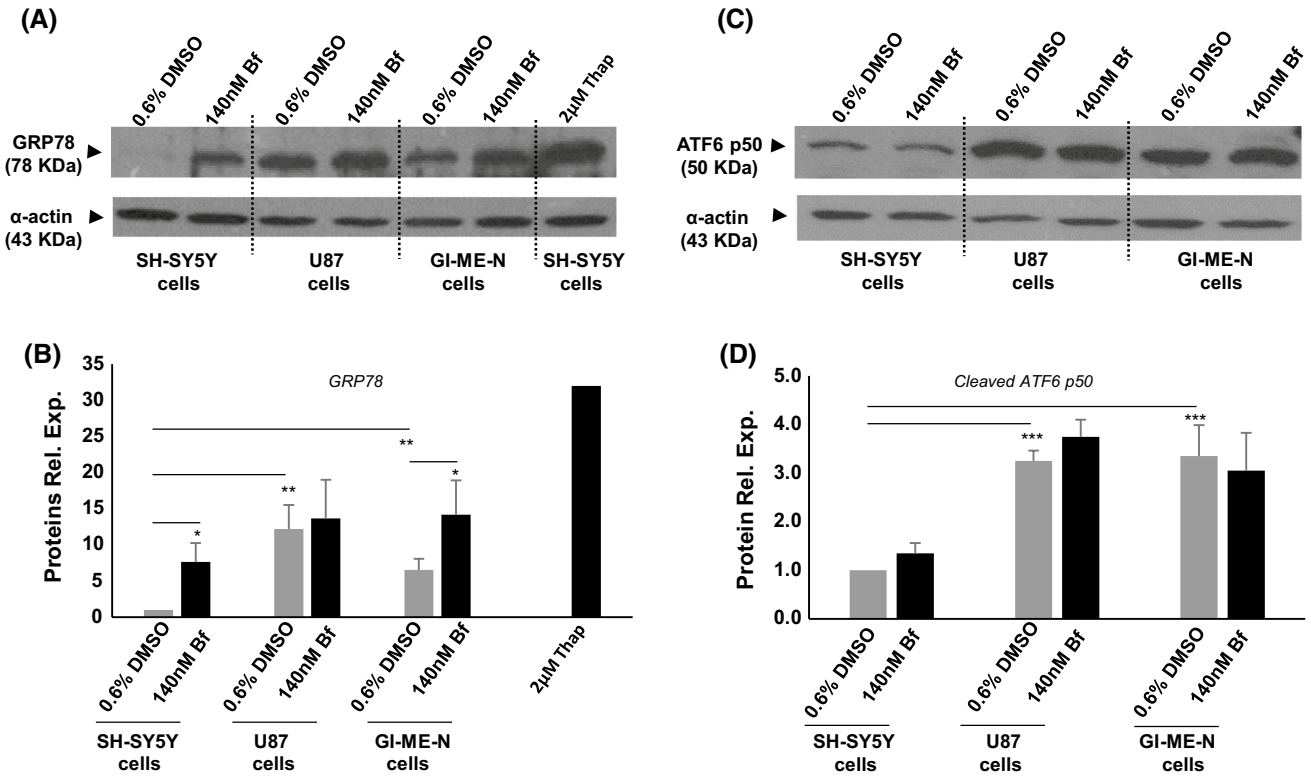


**Fig. 2** ATF6 proteolytic cleavage and GRP78 protein expression upon UCB treatment in three different cell lines. **a** Representative Immunoblot of GRP78 in SH-SY5Y, U87 and GI-ME-N cells treated with 0.6 % DMSO and 140 nM Bf for 24 h. SH-SY5Y cells treated with 2 μM thapsigargin (Thap) for 24 h were used as positive control. **b** The optical density of each band of GRP78 was normalized to α-actin and represented as relative to SH-SY5Y cells treated with DMSO. **(C)** Representative Immunoblot of ATF6 cleaved form in SH-SY5Y, U87 and GI-ME-N cells treated with 0.6 % DMSO and 140 nM Bf for 24 h. **d** The optical density of each band of cleaved ATF6 was normalized to α-actin and represented as relative to SH-SY5Y cells treated with DMSO. Data are the mean ± SD of three independent experiments (*$P < 0.05$, **$P < 0.01$, ***$P < 0.001$)

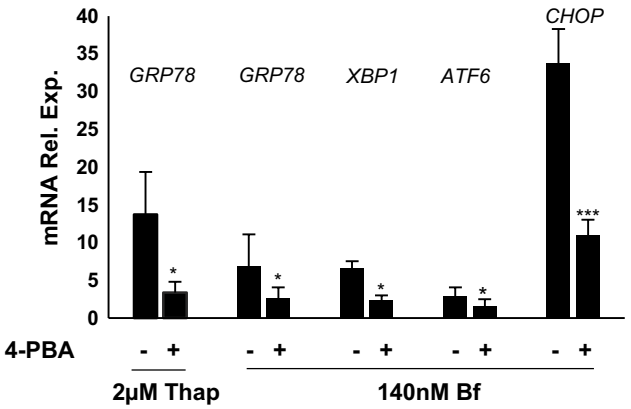


**Fig. 3** Effect of ER stress inhibitor (4-PBA) on the mRNA induction of ER stress genes by UCB in SH-SY5Y cells. mRNA expression of GRP78, XBP1, ATF6 and CHOP in SH-SY5Y cells exposed to 140 nM Bf for 8 h in the presence (+) or absence (−) of 2 mM 4-PBA. Expression was expressed as relative to cells treated with 0.6 % DMSO in the presence or absence of 4-PBA. Cells treated with 2 μM thapsigargin (Thap) for 8 h were used as positive control. Data are the mean ± SD of four independent experiments (*$P < 0.05$, ***$P < 0.001$)

## UCB induces inflammatory response and activates NFκB pathway

As several studies demonstrated the neuro-inflammatory effects of toxic UCB, we firstly analyzed the neuro-inflammatory effects of UCB in SH-SY5Y cells. Compared to DMSO-treated cells, UCB induced the mRNA expression of TNFα (30-folds and 6-folds) and IL-8 (57-folds and 203-folds) (Fig. 5a, b) at 8 and 24 h, respectively; IL-6 is not expressed in SH-SY5Y (data not shown). The secretion of TNFα protein was increased 8 h after UCB exposure (24 pg/mL) compared to DMSO-treated cells (8 pg/mL) and returned to basal levels after 24 h of treatment (Fig. 5c). IL-8 protein was detected only in the supernatants of cells treated with 140 nM Bf for 24 h (18 pg/mL) (Fig. 5d). SH-SY5Y cells treated with 140 nM Bf for 8 h showed an up-regulation of NFκB mRNA (3.5-folds) (Fig. 5e). In the presence of a potent NFκB inhibitor (PDTC) (Schreck et al. 1992), TNFα induction by UCB was unchanged, while IL-8 induction was reduced by 90 % (Fig. 5f, g). To confirm activation by UCB of the

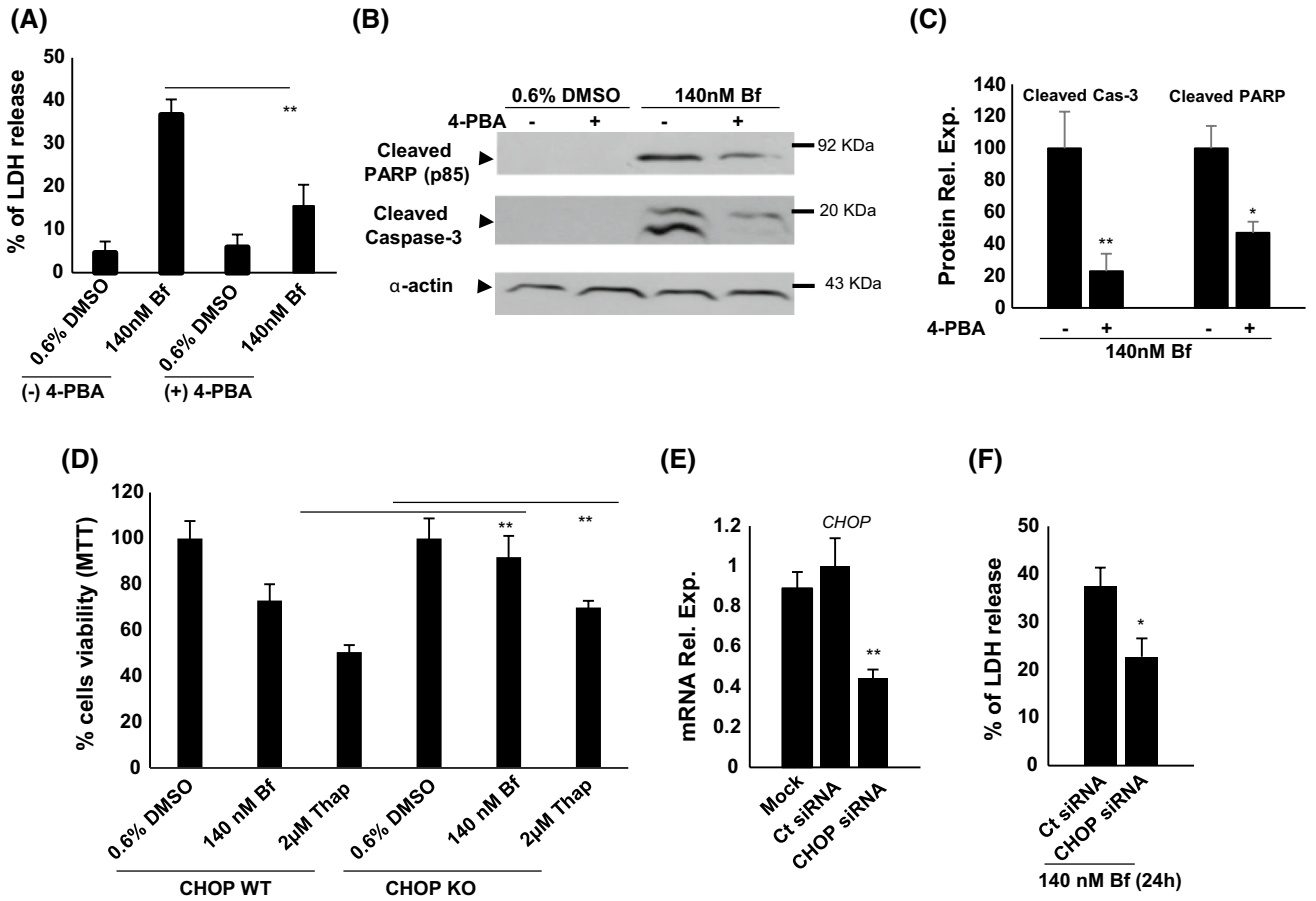


**Fig. 4** Effects of 4-PBA and CHOP knockout on cells death upon UCB exposure. **a** LDH release in SH-SY5Y cells exposed to 140 nM Bf or relative controls (0.6 % DMSO) for 24 h in the presence (+) or in the absence (−) of 4-PBA. Percent of dead cells was normalized to cells treated with lysis buffer to obtain 100 % of LDH release. **b** Representative Immunoblot of cleaved PARP and cleaved caspase-3 in SH-SY5Y cells exposed to 0.6 % DMSO or 140 nM Bf for 24 h in the presence (+) or absence (−) of 4-PBA. **c** The optical density of the two bands of cleaved caspase-3 and the band of cleaved PARP were normalized to α-actin and represented as relative to control. **d** MTT assay performed in CHOP WT and CHOP KO MEF cells treated with 0.6 % DMSO, 140 nM Bf or 2 μM thapsigargin (positive control) for 24 h. Significance relates to CHOP WT cells that received the same treatments. **e** CHOP siRNA efficiency in SH-SY5Y. Cells were transfected with CHOP siRNA, control siRNA (Ct siRNA) or in absence of siRNA (Mock) for 48 h and then CHOP mRNA expression was analyzed by qRT-PCR. **f** LDH release in SH-SY5Y cells transfected with CHOP siRNA or control siRNA (Ct siRNA) and exposed to 140 nM Bf for 24 h. Percent of dead cells was normalized to control siRNA-transfected cells treated with lysis buffer to obtain 100 % of LDH release. Data are the mean ± SD of four independent experiments (*$P < 0.05$, **$P < 0.01$)

NFκB pathway, we analyzed the transcriptional activity of NFκB toward the human IL-8 promoter using luciferase reporter gene assay. Cells were transfected with human IL-8 constructs containing the NFκB binding site (hIL-8/Luc) or the mutant NFκB enhancer (hIL-8/Luc ΔNF-kB) and then treated with 0.6 % DMSO (negative control), 100 ng/mL LPS (positive control) or 140 nM Bf for 24 h. Relative to DMSO-treated cells, UCB and LPS stimulated IL-8 luciferase activity (3.2- and 2.4-folds, respectively) in cells transfected with hIL-8/Luc construct while luciferase activity decreased in cells transfected with the hIL-8/Luc ΔNF-kB mutant construct (1.6- and 0.9-folds, respectively) (Fig. 5h). NFκB, TNFα and IL-8 mRNA expression was also analyzed in GI-ME-N and U87 cells after 8 h of 140 nM Bf exposure. UCB induced mRNA expression of NFκB (twofolds), TNFα (30-folds) and IL-8 (105-folds) in GI-ME-N cells while no changes were detected in U87 cells (data not shown).

## ER stress inhibition and PERK siRNA reduce IL-8 induction by UCB

To analyze the contribution of ER stress in mediating the inflammatory response, TNFα and IL-8 mRNA expression was analyzed in SH-SY5Y cells exposed to 140 nM Bf for 8 h in the presence of 4-PBA and 4-PBA reduced only IL-8 induction by 80 % (Fig. 6a). To test the contribution of PERK signaling in the induction of TNFα and IL-8, we

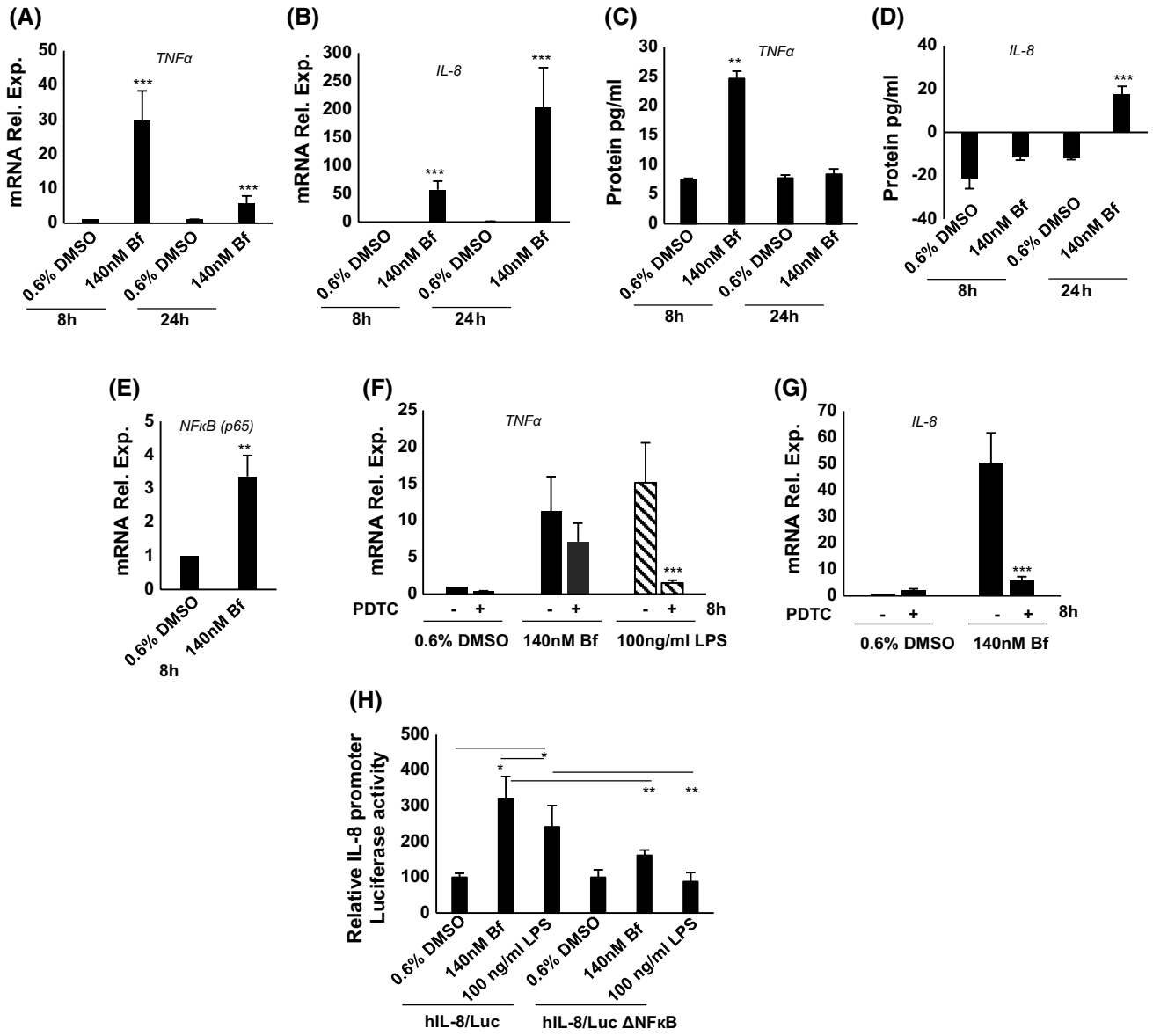


**Fig. 5** Effects of UCB on the inflammatory response in SH-SY5Y cells. **a** and **b** TNFα and IL-8 protein release analyzed by Instant ELISA Kit in the supernatant of cells exposed to 140 nM Bf or to DMSO at the indicated time. Significance relates to cells treated with DMSO. (**c**) mRNA expression of NF-kB after 8 h of 140 nM Bf or DMSO exposure. Expression was expressed as relative to cells treated with DMSO. (**d**) Luciferase reporter gene assay. Cells were transfected with the human constructs of IL-8 promoter under the control of luciferase: hIL-8/Luc. constructs contain NF-kB binding site or hIL-8/Luc ΔNFκB constructs contain the mutant NFκB enhancer. 24 h post-transfection, cells were treated with 0.6 % DMSO, 140 nM Bf or 100 ng/mL LPS (positive control) for 24 h. Firefly luciferase activity was normalized to the Renilla luciferase activity and represented relative to DMSO-treated controls

used specific siRNA to knockdown PERK mRNA expression. PERK siRNA (50 nM) down-regulated PERK mRNA to about 70 % as compared to control siRNA (50 nM) (Fig. 6b). After 48 h of transfection, cells were treated with 140 nM Bf for additional 8 h. The UCB-related induction of IL-8 mRNA, but not of TNFα, was decreased by 75 % in the PERK siRNA-transfected cell compared to control siRNA-transfected cells (Fig. 6c).

## Discussion and conclusion

Cell fate in response to ER stress mainly depends on the level of ER stress. Although the initial role of ER stress is to provide cell survival, chronic ER stress is associated with cell injury and with the activation of a complex of pro-apoptotic signaling (CHOP induction, caspases activation, disruption of $Ca^{2+}$ homeostasis, oxidative stress and

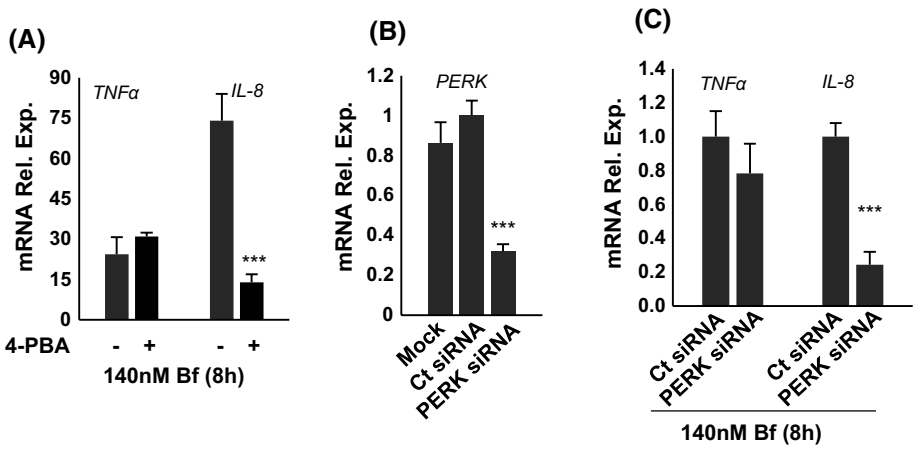


**Fig. 6** Effects of ER stress inhibition on TNFα and IL-8 mRNA induction by UCB in SH-SY5Y cells **a** mRNA expression of TNFα and IL-8 in SH-SY5Y exposed to 140 nM Bf for 8 h in the presence (+) or absence (−) of 4-PBA. Expression was expressed as relative to cells treated with 0.6 % DMSO in the presence or absence of 4-PBA. **b** PERK siRNA efficiency. SH-SY5Y cells were transfected with PERK siRNA, control siRNA (Ct siRNA) or in absence of siRNA (Mock) for 48 h and PERK mRNA knockdown efficiency was analyzed by qRT-PCR. **c** mRNA expression of TNFα and IL-8 in SH-SY5Y treated with 140 nM Bf for 8 h after 48 h of siRNA transfection. Expression was expressed as relative to Ct siRNA-transfected cells treated with Bf. Data are the mean ± SD of three (reporter gene assay) or four (all the others) independent experiments (*$P < 0.05$, **$P < 0.01$, ***$P < 0.001$)

inflammation) (Lai et al. 2007; Chaudhari et al. 2014). ER has a very specialized environment that allows proper protein folding, and it is extremely sensitive to toxic insults and stress conditions (Schönthal 2012). UCB once entered into the cells is shuttled to the ER, suggesting that—in case of hyperbilirubinemia—ER may become "a sink" and may represent an early target to UCB toxicity.

Few in vitro studies showed an up-regulation of ER stress-related genes by toxic concentration of UCB (Calligaris et al. 2009; Oakes and Bend 2010; Müllebner et al. 2015; Barateiro et al. 2012). Calligaris et al. (Calligaris et al. 2009) showed that 24 h of 140 nM Bf treatment is able to trigger unconventional splicing of XBP1 and cytoplasm/nuclear shuttling of CHOP in SH-SY5Y cells. Recently, we observed the induction of ATF3 after 4 h of UCB exposure in SH-SY5Y neuronal cells, indicating the activation of ER stress as an early event in the UCB-induced cytotoxicity (Qaisiya 2014). In the present study, we performed an in vitro comparative study using two neuronal cell lines (undifferentiated SH-SY5Y and differentiated GI-ME-N cells) and one astrocytoma cell line (U87 cells) analyzing the ER stress and its contribution to inflammation and cell death induced by UCB.

When exposed to increasing toxic concentrations of UCB, U87 astrocytoma cells maintain their viability even at the highest concentration of UCB. Undifferentiated SH-SY5Y neuronal cell line appears to be the most sensitive cells with a clear dose-dependent increase in LDH release, while differentiated neuronal GI-ME-N cells show comparable LDH release in spite of increasing UCB concentration (Fig. 1a). Differentiation of SH-SY5Y cells increases their resistance to UCB toxicity since differentiated cells showed 85 % of cells viability at 140 nM Bf or 300 nM Bf exposure, while the viability of the undifferentiated cells was 66 and 40 %, respectively (data not shown). These data, in line with others (Falcão et al. 2006; Brito et al. 2008), indicate that neuronal cells are more sensitive to UCB toxicity than glial cells, and that the neuronal UCB toxicity varies with the differentiation state. Despite a different toxicity, all the three cell types accumulate UCB in a time-dependent manner (Fig. 1b) and in the hyperbilirubinemic Gunn rat, different brain regions have the same bilirubin content but a different neurotoxicity profile (Gazzin et al. 2012). Collectively, both the in vitro and in vivo data exclude that the differential UCB toxicity is due to the different intracellular accumulation of UCB and suggest the presence of specific protective pathways and different intracellular signaling activation. UCB oxidation is one method of detoxification. Brain UCB oxidizing activity is lower in immature than in more mature brain and in pure neuronal membranes compared to mixed glial/neuronal source (Hansen and Allen 1997), and cytochromes P450 activity was demonstrated in rat primary astrocytes cultures (Gambaro et al. 2016). Since P450 is involved in UCB oxidation, the different expression of the enzyme may account for the different toxic effect in neurons and astrocytes of UCB.

However, in addition to the different bilirubin oxidation levels between neurons and astrocytes, we hypothesized that neurons and astrocytes could also present a different ER stress response to UCB. The chaperone GRP78 is the putative marker of ER stress (Lee 2005). We observed a clear difference of GRP78 proteins basal expression

between the three cell lines with U87 cells showing the highest GRP78 protein level followed by GI-ME-N as compared to SH-SY5Y cells (Fig. 2c, d). Several studies showed that overexpression of GRP78 in neuronal cells provides protections against ER stress and apoptosis (Kudo et al. 2007), which may explain the greater resistance of U87 and GIMEN cells to UCB toxicity compared to SH-SY5Y cells.

Regarding ER stress induction by UCB, analysis of ER stress markers showed an early up-regulation of CHOP, ATF6 and GRP78 mRNA expression (Table 2) in both neuronal cells, but not in the astrocytoma cells. The GRP78 induction only in neuronal cells was confirmed at the protein level (Fig. 2a, b), while the proteolytic cleavage of ATF6 was not changed in any cell line by UCB treatment (Fig. 2c, d) indicating that ATF6 sensor is not activated by UCB. Since the unconventional splicing of XBP1 was previously demonstrated in SH-SY5Y cells (Calligaris et al. 2009), we may conclude that UCB causes ER stress in neuronal cells mainly via PERK and IRE1 branches.

The cause of the ER stress induction by UCB is unknown. Primary culture of neurons showed an increase in intracellular $Ca^{+2}$ when exposed to toxic concentration of UCB (Zhang et al. 2010) which may derived either from extracellular influx or from intracellular stores release (Watchko 2006), and contribute to ER dysfunction (Paschen and Mengesdorf 2005; Ruiz et al. 2009). SH-SY5Y cells treated with 140 nM Bf in the presence of intracellular $Ca^{+2}$ chelator BAPTA decreased the induction of GRP78 by 50 %, suggesting the presence of $Ca^{+2}$ signaling that influences the expression of ER stress marker GRP78 (data not shown). We also detected an increment in oxidative stress (Qaisiya 2014) and metabolic changes (Calligaris et al. 2009), two events both contributing to ER stress response activation (Kaufman 1999; Hamanaka et al. 2005; Harding et al. 2000). Finally, due to its particular chemical properties, high levels of UCB may disrupt protein folding by direct interactions (Müllebner et al. 2015). Considering the role of ER stress in neuronal cell injury (Lindholm et al. 2006), we treated SH-SY5Y cells with UCB in the presence of 4-PBA, an ER stress inhibitor acting as chemical chaperone with significant therapeutic value (Mimori et al. 2012). Interestingly, 4-PBA significantly reduced the mRNA up-regulation of ER stress markers by UCB, indicating their induction via UPR signaling (Fig. 3).

4-PBA also decreased cells injury/apoptosis and reduced the amount of the cleaved caspase-3 and its substrate the cleaved PARP (Fig. 4a–c), suggesting an important role of ER stress in mediating caspase-3 activation, PARP cleavage and apoptosis by UCB. It has been reported that UCB-induced ER stress involves activation of caspase-12 (Oakes and Bend 2010) and $Ca^{2+}$-dependent protease enzyme (Calpain) (Barateiro et al. 2012), both of which may subsequently activate downstream caspase-3 (Lai et al. 2007). JNK activation by UCB was suggested to be associated with mitochondrial dysfunction and apoptosis in astrocytes, immature neurons and oligodendrocyte precursors cells (Barateiro et al. 2012; Fernandes et al. 2007; Vaz et al. 2011). However, under ER stress conditions the role of JNK in mediating cells survival or apoptosis is still controversial which may explained by the selective interaction between different JNK isoforms with different transcription factors (Raciti et al. 2012). We exposed SH-SY5Y cells to UCB in the presence of the JNK inhibitor (SP 600125), but we did not detect any change in the MTT and LDH assays (data not shown). Another major event responsible for the switch between pro-survival and pro-apoptotic responses under chronic ER stress is the induction of CHOP (Urra et al. 2013). Animals and cells derived from mice that are null-zygous for the *chop* gene (CHOP KO) are resistant to insults resulting in ER stress-mediated cell death (Zinszner et al. 1998). To test the role of CHOP in UCB-induced cell toxicity, CHOP KO and WT MEF cells were treated with toxic Bf concentration. CHOP KO cells showed 20 % increase in cells viability compared to CHOP WT cells, pointing to important role for CHOP in ER stress-induced cell toxicity by UCB (Fig. 4d). To confirm this data in neuronal cells, we transfected SH-SY5Y cells with CHOP siRNA that reduced cell toxicity by 40 % (Fig. 4f). It is worth to notice the different behavior of CHOP induction by UCB between undifferentiated SH-SY5Y and differentiated GI-ME-N cells. In the SH-SY5Y cells, CHOP mRNA induction occurs after 4 h of UCB treatment (sixfolds) but it is strongly increased after 24 h (93-fold) while GI-ME-N cells showed a decrease in the mRNA induction at 24 h (sixfolds) compared to 4 h (19-folds) (Table 2). Interestingly, we observed that the mRNA induction of CHOP by UCB is 75 % lower in the differentiated SH-SY5Y cells compared to the undifferentiated SH-SY5Y cells (data not shown), suggesting that ER responds to UCB toxic load by differently modulating CHOP induction during differentiation process. This may contribute to explain the differential toxicity profile between differentiated and undifferentiated neuronal cells. We suggest that ER stress may also have a role in the toxicity associated with exposure of premature neural cells to UCB and may contribute to better understand the high risk of premature infants to develop UCB neurotoxicity (Notter and Kendig 1986; Conlee and Shapiro 1997; Rhine et al. 1999).

Sustained ER stress elicits inflammatory response through complex mechanisms. We detected the neuroinflammatory effects of UCB by the induction of TNFα, IL-8 and NFκB in SH-SY5Y cells (Fig. 5a–e), in line with previous data (Falcão et al. 2006; Brites 2012; Yueh

et al. 2014). NFκB plays an important role in the activation of inflammatory response genes, and studies showed its activation by UCB (Brites 2012; Yueh et al. 2014). Indeed, cells transfected with human IL-8 promoter mutant for NFκB reduced the promoter activity, confirming the transcriptional activation of NFκB toward IL-8 by UCB (Fig. 5h). To analyze the contribution of ER stress in the inflammatory response, we used the general ER stress inhibitor 4-PBA, which significantly reduced the induction of IL-8 by UCB (Fig. 6a). To identify the link between ER stress and inflammation, we explored PERK signaling since (a) induction of ATF3 and CHOP after 4 h suggests PERK sensor activation for first; and (b) PERK plays a critical role in the regulation of inflammatory response under ER stress (Deng et al. 2004; Tam et al. 2012). Cells transfected with PERK siRNA reduced the up-regulation of IL-8 by 75 % (Fig. 6c). These data indicate that ER stress-induced IL-8 expression upon UCB treatment is regulated by the upstream NFκB/PERK axis.

The present data show that the neuronal cells are more susceptible to UCB toxicity than astrocyte cells, although UCB accumulates in both cell types to the same extent. Of notice, UCB induces ER stress only in neuronal cells and not in astrocytes. The sensitivity of neuronal cells to UCB toxicity correlates with high level of CHOP expressions, and they are more pronounced in undifferentiated than in differentiated cells with important potential implications in the developing brain during the neonatal period. ER stress inhibitor and deletion of CHOP greatly reduced UCB-induced cytotoxicity. UCB-induced ER stress is associated with up-regulation of IL-8, which is transcriptionally induced by NFκB and regulated by PERK signaling (Fig. 7). Collectively our data suggest that targeting ER stress may represent a potential therapeutic approach to decrease cytotoxicity induced by high concentrations of UCB.

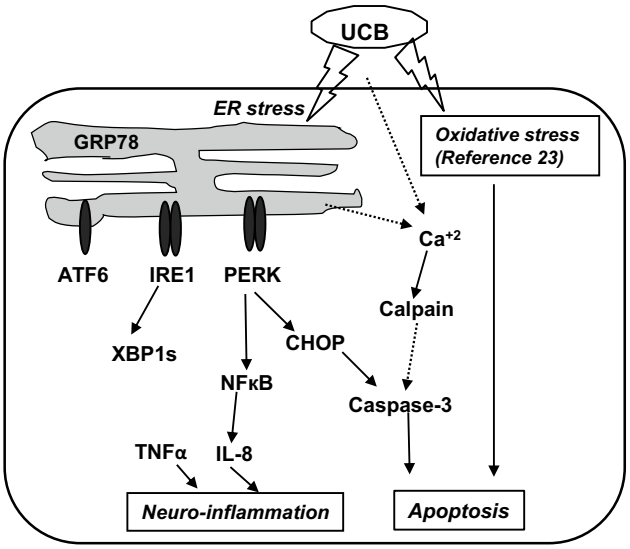


**Fig. 7** Proposed model of cellular signaling associated with UCB toxicity in SH-SY5Y cells. UCB-induced ER stress activates PERK and IREα sensors, leads to apoptosis through CHOP induction and increases IL-8 expression via NFκB/PERK signaling

**Acknowledgments** Authors want to thank Melania Zanchetta for performing plasmid amplification. Authors also thank AREA Science Park for supporting Mohammed Qaisiya fellowship. This work was supported in part by and intramural grant from Fondazione Italiana Fegato, ONLUS and by grant RVO VFN64165 from the Czech Ministry of Health, and by grant KONTAKT LH15097 from the Czech Ministry of Education.

**Compliance with ethical standards**

**Conflict of interest** The authors report no conflicts of interest. The authors alone are responsible for the content and writing of this article.

## References

Abu-Bakar A, Moore MR, Lang MA (2005) Evidence for induced microsomal bilirubin degradation by cytochrome P450 2A5. Biochem Pharmacol 70:1527–1535

Ahlfors CE, Wennberg RP, Ostrow JD, Tiribelli C (2009) Unbound (free) bilirubin: improving the paradigm for evaluating neonatal jaundice. Clin Chem 55:1288–1299

Barateiro A, Vaz AR, Silva SL, Fernandes A, Brites D (2012) ER stress, mitochondrial dysfunction and calpain/JNK activation are involved in oligodendrocyte precursor cell death by unconjugated bilirubin. Neuromolecular Med 14:285–302

Brites D (2012) The evolving landscape of neurotoxicity by unconjugated bilirubin: role of glial cells and inflammation. Front Pharmacol 3:88

Brito MA et al (2008) Unconjugated bilirubin differentially affects the redox status of neuronal and astroglial cells. Neurobiol Dis 29:30–40

Calligaris R et al (2009) A transcriptome analysis identifies molecular effectors of unconjugated bilirubin in human neuroblastoma SH-SY5Y cells. BMC Genom 10:543

Cesaratto L et al (2013) Specific inhibition of the redox activity of Ape1/Ref-1 by E3330 blocks Tnf-A-induced activation of Il-8 production in liver cancer cell lines. PLoS One 8(8):e70909

Chaudhari N, Talwar P, Parimisetty A, Lefebvre d'Hellencourt C, Ravanan P (2014) A molecular web: endoplasmic reticulum stress, inflammation, and oxidative stress. Front Cell Neurosci 8:213

Conlee JW, Shapiro SM (1997) Development of cerebellar hypoplasia in jaundiced Gunn rats: a quantitative light microscopic analysis. Acta Neuropathol 93:450–460

Deng J et al (2004) Translational repression mediates activation of nuclear factor kappa B by phosphorylated translation initiation factor 2. Mol Cell Biol 24:10161–10168

Falcão AS, Fernandes A, Brito MA, Silva RFM, Brites D (2006) Bilirubin-induced immunostimulant effects and toxicity vary with neural cell type and maturation state. Acta Neuropathol 112:95–105

Fernandes A, Falcão AS, Silva RFM, Brito MA, Brites D (2007) MAPKs are key players in mediating cytokine release and cell death induced by unconjugated bilirubin in cultured rat cortical astrocytes. Eur J Neurosci 25:1058–1068

Gambaro SE, Robert MC, Tiribelli C, Gazzin S (2016) Role of brain cytochrome P450 mono-oxygenases in bilirubin oxidation-specific induction and activity. Arch Toxicol 90:279–290

Garg AD et al (2012) ER stress-induced inflammation: does it aid or impede disease progression? Trends Mol Med 18:589–598
Gazzin S et al (2012) Bilirubin accumulation and Cyp mRNA expression in selected brain regions of jaundiced Gunn rat pups. Pediatr Res 71:653–660
Hamanaka RB, Bennett BS, Cullinan SB, Diehl JA (2005) PERK and GCN2 contribute to eIF2alpha phosphorylation and cell cycle arrest after activation of the unfolded protein response pathway. Mol Biol Cell 16:5493–5501
Hansen TW, Allen JW (1997) Oxidation of bilirubin by brain mitochondrial membranes–dependence on cell type and postnatal age. Biochem Mol Med 60:155–160
Harding HP et al (2000) Regulated translation initiation controls stress-induced gene expression in mammalian cells. Mol Cell 6:1099–1108
Hasnain SZ, Lourie R, Das I, Chen AC-H, McGuckin MA (2012) The interplay between endoplasmic reticulum stress and inflammation. Immunol Cell Biol 90:260–270
Hitomi J et al (2004) Apoptosis induced by endoplasmic reticulum stress depends on activation of caspase-3 via caspase-12. Neurosci Lett 357:127–130
Hotamisligil GS (2010) Endoplasmic reticulum stress and the inflammatory basis of metabolic disease. Cell 140:900–917
Kamisako T et al (2000) Recent advances in bilirubin metabolism research: the molecular mechanism of hepatocyte bilirubin transport and its clinical relevance. J Gastroenterol 35:659–664
Kaufman RJ (1999) Stress signaling from the lumen of the endoplasmic reticulum: coordination of gene transcriptional and translational controls. Genes Dev 13:1211–1233
Kudo T et al (2007) A molecular chaperone inducer protects neurons from ER stress. Cell Death Differ 15:364–375
Lai E, Teodoro T, Volchuk A (2007) Endoplasmic reticulum stress: signaling the unfolded protein response. Physiology 22:193–201
Lee AS (2005) The ER chaperone and signaling regulator GRP78/BiP as a monitor of endoplasmic reticulum stress. Methods 35:373–381
Lindholm D, Wootz H, Korhonen L (2006) ER stress and neurodegenerative diseases. Cell Death Differ 13:385–392
Malhotra JD, Kaufman RJ (2007) Endoplasmic reticulum stress and oxidative stress: a vicious cycle or a double-edged sword? Antioxid Redox Signal 9:2277–2293
Mimori S et al (2012) Protective effects of 4-phenylbutyrate derivatives on the neuronal cell death and endoplasmic reticulum stress. Biol Pharm Bull 35:84–90
Müllebner A, Moldzio R, Redl H, Kozlov AV, Duvigneau JC (2015) Heme degradation by heme oxygenase protects mitochondria but induces ER stress via formed bilirubin. Biomolecules 5:679–701
Neve EPA, Ingelman-Sundberg M (2010) Cytochrome P450 proteins: retention and distribution from the endoplasmic reticulum. Curr Opin Drug Discov Devel 13:78–85
Notter MF, Kendig JW (1986) Differential sensitivity of neural cells to bilirubin toxicity. Exp Neurol 94:670–682
O'Brien MA, Moravec RA, Riss TL (2001) Poly (ADP-ribose) polymerase cleavage monitored in situ in apoptotic cells. Biotechniques 30:886–891
Oakes GH, Bend JR (2010) Global changes in gene regulation demonstrate that unconjugated bilirubin is able to upregulate and activate select components of the endoplasmic reticulum stress response pathway. J Biochem Mol Toxicol 24:73–88
Ostrow JD, Pascolo L, Tiribelli C (2003) Reassessment of the unbound concentrations of unconjugated bilirubin in relation to neurotoxicity in vitro. Pediatr Res 54:98–104
Oyadomari S, Mori M (2004) Roles of CHOP/GADD153 in endoplasmic reticulum stress. Cell Death Differ 11:381–389
Paschen W, Mengesdorf T (2005) Endoplasmic reticulum stress response and neurodegeneration. Cell Calcium 38:409–415
Qaisiya M, Zabetta CDC, Bellarosa C, Tiribelli C (2014) Bilirubin mediated oxidative stress involves antioxidant response activation via Nrf2 pathway. Cell Signal 26:512–520
Raciti M, Lotti LV, Valia S, Pulcinelli FM, Di Renzo L (2012) JNK2 is activated during ER stress and promotes cell survival. Cell Death Dis 3:e429
Rhine WD, Schmitter SP, Yu AC, Eng LF, Stevenson DK (1999) Bilirubin toxicity and differentiation of cultured astrocytes. J Perinatol Off J Calif Perinat Assoc 19:206–211
Roca L et al (2006) Factors affecting the binding of bilirubin to serum albumins: validation and application of the peroxidase method. Pediatr Res 60:724–728
Ruiz A, Matute C, Alberdi E (2009) Endoplasmic reticulum Ca2 + release through ryanodine and IP3 receptors contributes to neuronal excitotoxicity. Cell Calcium 46:273–281
Schönthal AH (2012) Endoplasmic reticulum stress: its role in disease and novel prospects for therapy. Scientifica (Cairo) 2012:857516
Schreck R, Meier B, Männel DN, Dröge W, Baeuerle PA (1992) Dithiocarbamates as potent inhibitors of nuclear factor kappa B activation in intact cells. J Exp Med 175:1181–1194
Schröder M, Kaufman RJ (2005) The mammalian unfolded protein response. Annu Rev Biochem 74:739–789
Shapiro SM (2004) Definition of the clinical spectrum of kernicterus and bilirubin-induced neurologic dysfunction (BIND). J Perinatol 25:54–59
Tam AB, Mercado EL, Hoffmann A, Niwa M (2012) ER stress activates NF-κB by integrating functions of Basal IKK activity, IRE1 and PERK. PLoS One 7:e45078
Tsang KY, Chan D, Bateman JF, Cheah KSE (2010) In vivo cellular adaptation to ER stress: survival strategies with double-edged consequences. J Cell Sci 123:2145–2154
Urra H, Dufey E, Lisbona F, Rojas-Rivera D, Hetz C (2013) When ER stress reaches a dead end. Biochim Biophys Acta 1833:3507–3517
Vaz AR et al (2011) Selective vulnerability of rat brain regions to unconjugated bilirubin. Mol Cell Neurosci 48:82–93
Walter P, Ron D (2011) The unfolded protein response: from stress pathway to homeostatic regulation. Science 334:1081–1086
Watchko JF (2006) Kernicterus and the molecular mechanisms of bilirubin-induced CNS injury in newborns. Neuromolecular Med 8:513–529
Watchko JF, Tiribelli C (2013) Bilirubin-induced neurologic damage–mechanisms and management approaches. N Engl J Med 369:2021–2030
Yueh M-F, Chen S, Nguyen N, Tukey RH (2014) Developmental onset of bilirubin-induced neurotoxicity involves Toll-like receptor 2-dependent signaling in humanized UDP-glucuronosyltransferase1 mice. J Biol Chem 289:4699–4709
Zelenka J, Leníček M (2008) High sensitive method for quantitative determination of bilirubin in biological fluids and tissues. J Chromatogr B 867:37–42
Zhang B, Yang X, Gao X (2010) Taurine protects against bilirubin-induced neurotoxicity in vitro. Brain Res 1320:159–167
Zinszner H et al (1998) CHOP is implicated in programmed cell death in response to impaired function of the endoplasmic reticulum. Genes Dev 12:982–995